MOLECULAR AND CELLULAR BIOLOGY, July 1996, p. 3545–3553 Vol. 16, No. 7
0270-7306/96/$04.00+0

NAB2, a Corepressor of NGFI-A (Egr-1) and Krox20, Is Induced by Proliferative and Differentiative Stimuli

JOHN SVAREN,[1] BRADLEY R. SEVETSON,[1] ELIZABETH D. APEL,[2] DRAZEN B. ZIMONJIC,[3] NICHOLAS C. POPESCU,[3] AND JEFFREY MILBRANDT[1]*

Departments of Pathology and Internal Medicine, Division of Laboratory Medicine,[1] and Department of Molecular Biology and Pharmacology,[2] Washington University School of Medicine, St. Louis, Missouri 63110, and Laboratory of Biology, National Cancer Institute, Bethesda, Maryland 20892-4255[3]

Received 26 January 1996/Returned for modification 12 March 1996/Accepted 5 April 1996

Previous work had identified a corepressor, NAB1, which represses transcriptional activation mediated by NGFI-A (also known as Egr-1, zif268, and Krox24) and Krox20. These zinc finger transcription factors are encoded by immediate-early genes and have been implicated in a wide variety of proliferative and differentiative processes. We have isolated and characterized another corepressor, NAB2, which is highly related to NAB1 within two discrete domains. The first conserved domain of NAB2 mediates an interaction with the R1 domain of NGFI-A. NAB2 represses the activity of both NGFI-A and Krox20, and its expression is regulated by some of the same stimuli that induce NGFI-A expression, including serum stimulation of fibroblasts and nerve growth factor stimulation of PC12 cells. The human NAB2 gene has been localized to chromosome 12q13.3-14.1, a region that is rearranged in several solid tumors, lipomas, uterine leiomyomata, and liposarcomas. Sequencing of the *Caenorhabditis elegans* genome has identified a gene that bears high homology to both NAB1 and NAB2, suggesting that NAB molecules fulfill an evolutionarily conserved role.

Transcriptional control plays a vital role in regulating fundamental cellular processes such as proliferation, differentiation, and cell death. Changes in gene expression are often effected by altering the expression level, activity, and/or nuclear localization of transcription factors that bind to promoter and enhancer regions. In addition, many transcription factors are regulated by direct interactions with other proteins which modulate the level of transcriptional activation.

A subclass of these cofactors, called corepressors, repress the activity of transactivators with which they interact, or even turn an activator into a transcriptional repressor. For example, the recruitment of Rb to a promoter by E2F disrupts interactions of nearby transcription factors with the basal transcription initiation complex (52). In this manner, the Rb-E2F complex represses transcription of several genes involved in DNA replication (51). Similarly, two recently discovered corepressors, N-CoR and SMRT, interact with the hinge regions of the thyroid and retinoic acid receptors and mediate repression by the unliganded forms of these receptors (7, 16). One of the best-characterized examples of corepression is the Ssn6/Tup1 complex in the yeast *Saccharomyces cerevisiae*. These two proteins are involved in transcriptional repression of a variety of genes, including genes regulated by glucose, DNA damage, mating type, and other signals. The Ssn6/Tup1 complex is recruited to glucose-repressible promoters by an interaction between Ssn6 and Mig1, a zinc finger DNA-binding protein. The repression function has been shown to reside in the Tup1 protein, because it will repress transcription in the absence of Ssn6 if tethered to a promoter by fusion to a DNA-binding domain (46). The Mig1 protein acts as a potent activator in an *ssn6* mutant strain, suggesting that Mig1 is a transactivator which is converted to a repressor by association with the Ssn6/Tup1 complex (45).

* Corresponding author. Mailing address: Department of Pathology, Campus Box 8118, 660 S. Euclid Ave., Washington University School of Medicine, St. Louis, MO 63110. Phone: (314) 362-4650. Fax: (314) 362-8756. Electronic mail address: jeff@milbrandt.wustl.edu.

Recent work from our laboratory has identified a novel corepressor, NAB1 (34), which represses transactivation by NGFI-A (24), a zinc finger transcription factor (also known as Egr-1, Krox24, and zif268) that is rapidly induced by a variety of extracellular stimuli (reviewed in reference 14). Mitogenic stimuli such as serum, platelet-derived growth factor, epidermal growth factor, and fibroblast growth factor result in sharply increased NGFI-A expression (5, 8, 20). In addition, NGFI-A is induced in response to agents which trigger differentiation pathways. NGFI-A expression is activated in nerve growth factor (NGF)-stimulated differentiation of PC12 cells (5, 6, 24), during differentiation of preosteoblastic cells (43), and also during B-cell maturation (39, 40, 48). NGFI-A has been implicated in macrophage differentiation (17) and regulation of growth arrest and apoptotic pathways in melanoma cell lines (26, 38) and has been shown to be required for regulation of pituitary gonadotropin production (19). Krox20, a closely related zinc finger protein, is also repressed by NAB1. Krox20 has been shown to play a critical role in both hindbrain segmentation and myelination of peripheral neurons (36, 44).

The existence of a corepressor of NGFI-A was first suggested by the finding that deletion of a segment of NGFI-A (termed the R1 domain) increases its activity more than 10-fold (15, 33). Subsequently, a screen of a yeast two-hybrid library by using the R1 domain identified NAB1, which was found to repress transactivation by NGFI-A and Krox20 in cotransfection experiments (34). In this study, we have identified a clone which codes for a protein, named NAB2, that bears sequence similarity to NAB1. We show that a NAB2 domain that is highly homologous to the corresponding region of NAB1 mediates an interaction between NAB2 and the NGFI-A R1 domain and that NAB2 also represses transactivation by NGFI-A. In contrast to NAB1, which is constitutively expressed, the expression level of NAB2 is increased by some of the same stimuli which rapidly induce NGFI-A, such as serum stimulation of fibroblasts and NGF stimulation of PC12 cells. These results suggest that NAB2 may play a role in downregu-

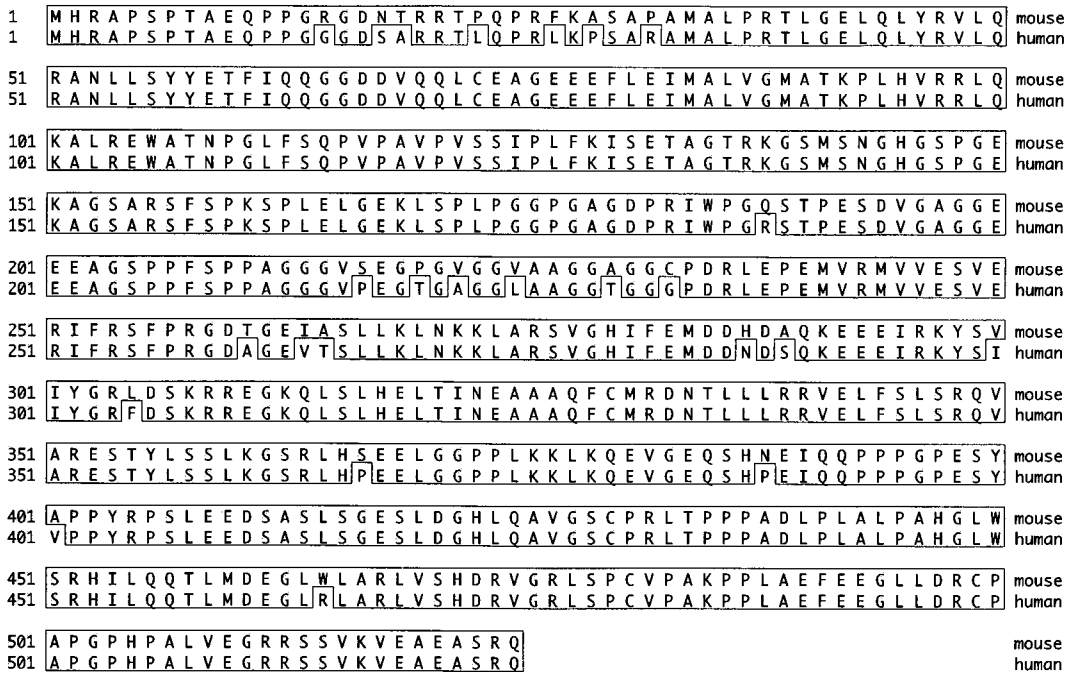

FIG. 1. Protein sequences of mouse and human NAB2. Residues which are identical are boxed.

lating the burst of NGFI-A activity which accompanies proliferative and differentiative signals.

MATERIALS AND METHODS

Isolation and sequence analysis of NAB2. Genomic P1 clones for mouse NAB1 were isolated by Genome Systems Inc. Sequencing of one these isolates showed that it was not NAB1 but rather a related gene which we called NAB2. The sequence was found to be almost identical to that of a human expressed sequence tag (Drop9) which had previously been deposited in GenBank (accession number X70991). We then isolated and sequenced NAB2 cDNA clones from mouse and human brain cDNA libraries. To determine the 5′ ends of the mouse and human mRNA sequences, we employed Marathon RACE (rapid amplification of cDNA ends) (Clontech) from mouse brain and human placental cDNAs, using two nested primers. The following primers were used according to the manufacturer's protocol for the initial PCR from mouse brain and human placental cDNA, respectively: CTTGAAAAGTGGGATGCTGGAGACGGGC and GAACTGGGCAGCAGCCTCGTTGATGGTG. A second PCR using nested primers, GCCAGCCTCACACAGCTGCTGTACATC (mouse) and CTTCT CTCCAAGTTCAAGGGGGC (human), on the products of the first reaction was used to obtain DNA fragments which were subcloned and sequenced. The addition of 5% dimethyl sulfoxide to both reactions increased the yield and size of the RACE PCR products, presumably because the 5′ untranslated region of NAB2 is relatively GC rich. All sequencing was performed with an Applied Biosystems model 373 automated DNA sequencer. Sequence comparisons were performed with BLAST (1), using the default parameters, to search the National Center for Biotechnology Information nonredundant protein and DNA databases. A search for protein motifs was performed with PROSITE (2). Sequence alignments were produced by using the DNASTAR program. Data on the genomic structure of mouse NAB2 will be published elsewhere (43a).

In the analysis of alternatively spliced NAB2 [NAB2 (A.S.)] (Fig. 7), the NAB2 ORF (open reading frame) was amplified from the indicated mouse cDNA samples by using the following primers: GGGCAGTGCTCGAAGCTTTAGCC and TCACTGCCGGCTGGCTTCTGCCTCCAC. The amplification produced two PCR products, corresponding to the full-length and alternatively spliced forms of NAB2, and both were subcloned and sequenced.

To create an expression vector for NAB2, the coding region of human NAB2 was amplified from human placental cDNA by PCR using primers derived from the Drop9 sequence (GCCAACCTCCTTTCCTACTATG and GGCGAAGCT TCTGCCGGCTGGCCTCAGCCTC). The resulting fragments (either full length or alternatively spliced) were combined with the 5′ end of the human cDNA obtained by RACE and cloned into the cytomegalovirus (CMV)-driven expression vector pCB6 (4) to make pCMVNAB2 and pCMVNAB2 (A.S.).

Yeast two-hybrid analysis. Fusions of the R1 domain of NGFI-A (or a version containing the Ile-293→Phe [I293F] mutation) with the Gal4 DNA-binding domain (DBD) have been described elsewhere (34). Fragments encompassing NAB conserved domain 1 (NCD1) of mouse NAB1 (residues 7 to 133) and NCD1 of *Caenorhabditis elegans* NAB (residues 1 to 100) were fused to the Gal4 DBD by subcloning them into *Eco*RI-*Bam*HI-digested pAS-1 (10). Fragments encompassing NCD1 of mouse NAB2 (residues 33 to 156), NCD1 of mouse NAB1 (residues 7 to 105), and the R1 domain of NGFI-A (residues 269 to 304) were fused to the Gal4 activation domain by subcloning them into *Not*I-*Xho*I-digested pBM2462 (21). These constructs were transformed into yeast strain YM2632 (*MAT***a** *ura3-52 his3-200 ade2-101 lys2-801 leu2-3,112 trp1-901 met2 gal4-542 gal80-538* Can^r, *LEU2*::*GAL1-lacZ*) provided by Mark Johnston, Washington University. The resulting strains were grown in selective medium, and *lacZ* expression from the *GAL1*-driven reporter gene was measured as previously described (32). Measurements are the averages of duplicate assays.

Transfections. Expression vectors for wild-type and mutant NGFI-A (I293F), Krox20, and the luciferase reporter construct containing two NGFI-A binding sites have been described previously (33). All transfections were performed in CV-1 cells essentially as described previously (33), using 20 ng of the NGFI-A or Krox20 expression plasmid, 500 ng of the luciferase reporter, 100 ng of a CMV-driven *lacZ* reporter, and the indicated amounts of the NAB2 expression plasmid. Bluescript plasmid (Stratagene) was added as required to make a total of 2 μg of DNA per transfection. Transfections were performed in six-well plates (Corning), using 6×10^4 cells per well. The luciferase activity of each sample was normalized to the β-galactosidase activity from the transfected *lacZ* reporter. The background activity from a transfection with the reporter gene alone was subtracted from the activities obtained in the presence of cotransfected NGFI-A.

Cell culture and RNA analysis. African green monkey CV-1 cells were cultured as previously described (27). Culture and stimulation of rat pheochromocytoma PC12 cells with NGF (a gift from Eugene Johnson, Washington University) were carried out as previously described (23, 24). Serum stimulation of murine fibroblast NIH 3T3 cells was performed by plating 7×10^5 cells onto 10-cm-diameter plates, culturing them for 72 h in Dulbecco modified Eagle medium containing 0.5% fetal calf serum, and stimulating them with medium containing 20% fetal calf serum. Plates were washed three times in phosphate-buffered saline (PBS) prior to harvest. RNA and protein were purified by using the Tri reagent (Molecular Research Center, Inc.) according to the manufacturer's instructions. RNA blot analysis was performed with 15 μg of total RNA per lane, using an *Msc*I fragment (1,000 bp) from the mouse NAB2 gene as a probe. The NGFI-A probe was a 1,400-bp *Nco*I-*Msc*I fragment. The hybridized blots were analyzed with a Molecular Dynamics PhosphorImager.

Antibody production and immunoblot analysis. Antibodies against NAB2 were prepared by immunizing rabbits with a peptide containing a cysteine followed by NAB2 residues 147 to 161 [NAB2 (147-161)] and coupled to keyhole limpet hemocyanin (Calbiochem). Affinity purification of NAB2 antibodies was carried out with the same peptide coupled to Sulfolink resin (Pierce). Protein samples were extracted from Tri reagent protein pellets with Laemmli buffer, boiled for 5 min prior to electrophoresis through a sodium dodecyl sulfate–10% polyacrylamide gel, and then transferred to nitrocellulose membranes (Midwest

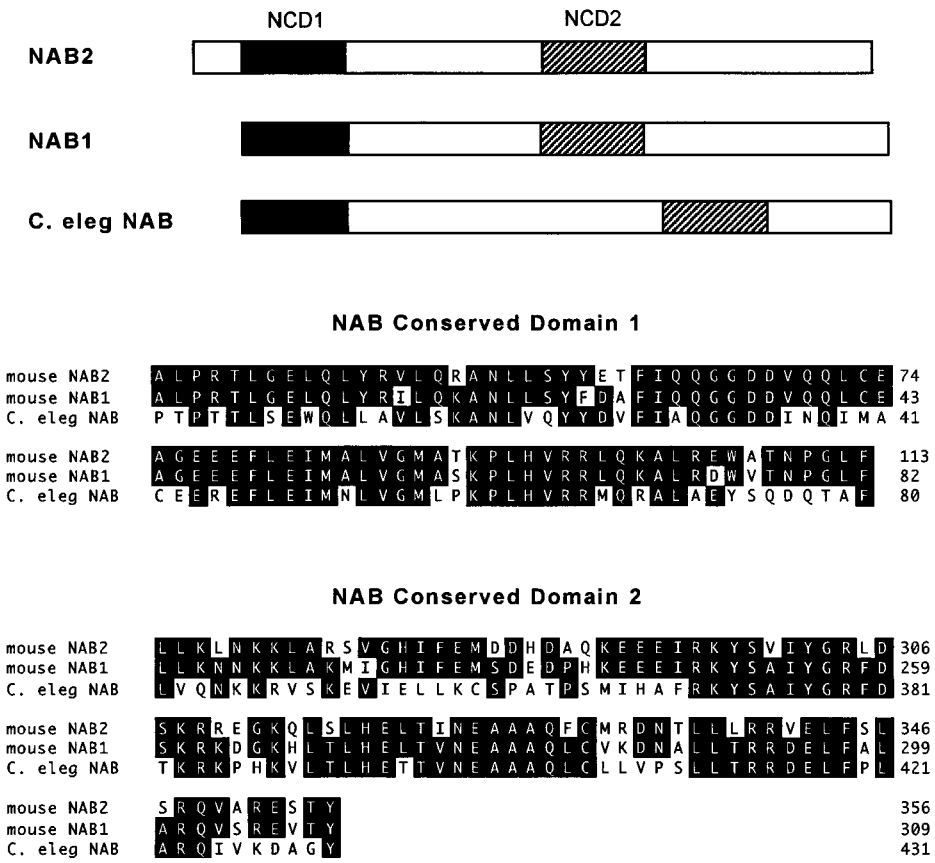

FIG. 2. NAB family members contain two evolutionarily conserved domains. The positions of NCD1 and NCD2 in NAB1, NAB2, and *C. elegans* (C. eleg) NAB are shown in the diagram. The sequences of NCD1 and NCD2 are shown below; amino acids that are identical in at least two of the three sequences are shaded. The *C. elegans* NAB sequence was derived from GenBank accession number Z50795.

Scientific). Membranes were blocked in Tris-buffered saline–Triton (TBST; 25 mM Tris-HCl [pH 7.4], 145 mM NaCl, 5 mM KCl, 1% Triton X-100) containing 5% milk prior to incubation with TBST containing 3% milk and 1 μg of affinity-purified NAB2 antiserum per ml. The protein blots were washed five times in TBST, incubated with horseradish peroxidase conjugated anti-rabbit immunoglobulin G (Jackson ImmunoResearch Laboratories, Inc., West Grove, Pa.), washed five times in TBST, and visualized by chemiluminescence detection (Amersham). An identical blot was incubated with the primary antibody in the presence of an excess of the NAB2 (147-161) peptide, and this competition assay confirmed the identity of the band as NAB2.

Immunofluorescence staining. NIH 3T3 cells were plated onto glass coverslips and starved of serum as described above. Medium containing serum was then added to the cells for 1 h. Both serum-starved and serum-stimulated cells were washed with PBS and then fixed for 20 min in PBS containing 1% paraformaldehyde, 100 mM L-lysine, 10 mM sodium *meta*-periodate, and 1% saponin. After being rinsed with PBS, cells were permeabilized for 10 min in 1% Triton X-100 in PBS, washed three times in PBS, and stored overnight in 10% fetal calf serum in PBS. Coverslips were inverted (cell side down) onto 50-μl drops of primary antibody and incubated for 2 h at 25°C. Primary antibodies were diluted 1:500 (NAB2 antibody) and 1:1,000 (NGFI-A antibody [9]) in PBS containing 10% fetal calf serum. Coverslips were washed three times with PBS, inverted onto 50-μl drops of donkey anti-rabbit secondary antibody Cys3 (Jackson ImmunoResearch Laboratories), diluted 1:4,000 in PBS with 10% fetal calf serum, and incubated for 1 h at 25°C. After three washes in PBS, coverslips were rinsed briefly in distilled water and mounted for fluorescence microscopy onto an antifading mountant. Parallel coverslips incubated with the secondary antibody alone showed negligible staining.

FISH localization. Chromosomes were obtained from peripheral lymphocyte cultures after methotrexate-thymidine release treatments and used for fluorescence in situ hybridization (FISH) as described previously (29, 54). The probes were labeled by nick translation with biotin-dUTP or digoxigen-11-dUTP. The slides were pretreated with RNase, denatured in 2× SSC (1× SSC is 0.15 M NaCl plus 0.015 M sodium citrate)–70% formamide for 2 min at 70°C, and hybridized with the DNA probe (200 ng) in 2× SSC–50% formamide–10% dextran sulfate–2× Denhardt's solution–1% Tween 20 for 18 h at 37°C. Biotin- and digoxigenin-labeled DNAs were detected by fluorescein isothiocyanate-conjugated avidin DCS (Vector Laboratories) and rhodamine-conjugated anti-digoxigenin (Boehringer Mannheim, Inc.), respectively. Chromosomes were counterstained with propidium iodide or diaminophenylindole (DAPI) and examined with an Olympus BH2 epifluorescence microscope. For each chromosomal spread, two consecutive 8-bit grayscale images (fluorescein isothiocyanate and propidium iodide, rhodamine, and DAPI) were recorded by an intensified charge-coupled device camera. To identify the labeled chromosomes, preparations were rehybridized with specific chromosome-painting probes (53), and previously observed labeled metaphases were rerecorded. Selected sets of corresponding raw images were then digitally enhanced for sharpness and contrast and merged (GeneJoin MaxPix). To precisely assign the location of fluorescent signals to specific chromosome bands, a recently reported method for direct visualization (55) was used. Final composite digital images were printed on a Tektronix Phase IISDX dye sublimation printer.

Nucleotide sequence accession numbers. The nucleotide sequences of mouse NAB2 (U47543), human NAB2 (U48361), mouse NAB1 (U47008), and human NAB1 (U47007) have been deposited in GenBank.

RESULTS

NAB1 and NAB2 are highly homologous within two domains. The NAB1 gene was previously identified through a yeast two-hybrid screen for proteins that interact with the R1 domain of NGFI-A (34). While isolating genomic clones of mouse NAB1, we obtained a clone that encodes a highly related protein. Using the sequence of the genomic clone, mouse and human brain cDNA libraries were screened, and the resulting cDNA clones were used, along with RACE PCR products (13), to determine the sequence of this protein, which we have named NAB2 (NGFI-A-binding protein 2). The mouse NAB2 ORF codes for a protein of 525 amino acids with a

TABLE 1. Interaction of NCD1 of NAB family members with the NGFI-A R1 domain in the yeast two-hybrid system

Gal4 DBD fusion[a]	Activation domain fusion[a]	β-Galactosidase activity (U)
NGFI-A	NAB1	150.5
NGFI-A (I293F)	NAB1	<0.5
NGFI-A	NAB2	83.5
NGFI-A (I293F)	NAB2	<0.5
NAB1	NGFI-A	61.2
C. elegans NAB	NGFI-A	16.0
No insert	NGFI-A	<0.5

[a] Residues included are described in Materials and Methods.

predicted molecular weight of 56,000 (Fig. 1). The amino acid sequence of NAB2 contains many charged residues (24%), and there is a high proportion of proline (10%), glycine (10%), and serine (9%) residues as well. Analysis of the protein sequence revealed a number of potential phosphorylation sites for cyclic AMP-dependent protein kinase, protein kinase C, casein kinase II, and proline-directed protein kinases. A partial cDNA of human NAB2 is present as an expressed sequence tag called Drop9 in the GenBank database.

NAB2 has significant homology to NAB1 within two blocks of approximately 100 amino acids each. In Fig. 2, the sequences of these domains are aligned with the corresponding domains of NAB1. In NCD1, 90% of the residues in a 79-amino-acid segment are identical in both NAB1 and NAB2. The sequence conservation of NCD1 is also apparent from the interspecies variation of NAB2 (Fig. 1). Although there are 25 amino acid changes between the mouse and human sequences of NAB2, none of these changes occur within NCD1. A second conserved domain of 90 amino acids (NCD2) which is 72% identical in NAB1 and NAB2 lies C terminal to a nonconserved spacer region. Apart from these two blocks of homology, the sequences of NAB1 and NAB2 have diverged considerably.

Recent sequencing of the *C. elegans* genome has uncovered a predicted ORF (accession number Z50795) which has high homology to NAB1 and NAB2 within the two conserved domains. As shown in Fig. 2, more than 40% of the residues in both NCD1 and NCD2 are identical in all three proteins, and those residues within the *C. elegans* protein that differ from the mouse counterparts tend to be conservative substitutions. Overall, the *C. elegans* NAB sequence is equally related to both NAB1 or NAB2, although the NCD2 domain seems to be more similar to that of NAB1. The fact that such high homology has been retained throughout evolution suggests that NAB-like proteins fulfill an important regulatory role and that interacting partners of NAB may also be conserved.

NAB2 interacts specifically with NGFI-A. The original NAB1 clone isolated from the yeast two-hybrid screen contained NCD1 (34), and subsequent experiments revealed that this domain interacts with the R1 domain of NGFI-A. Because the sequence of the NAB2 NCD1 closely resembles that of NAB1, we tested whether NAB2 would also interact with NGFI-A in the yeast two-hybrid interaction assay (11, 12). Plasmids expressing a fusion of the NAB2 NCD1 with the activation domain of Gal4, and a fusion of the NGFI-A R1 domain with the Gal4 DBD, were constructed. Both plasmids were transformed into a yeast strain containing an integrated reporter gene (*lacZ*) with four binding sites for Gal4 in its promoter. Coexpression of both plasmids resulted in activation of the *lacZ* reporter gene well above background levels (Table 1). Quantification of the *lacZ* expression showed that it was comparable to that resulting from the two-hybrid interaction between the NCD1 of NAB1 and the NGFI-A R1 domain.

Previous work had identified a point mutation (I293F) in the R1 domain which increases the activity of NGFI-A approximately 10-fold relative to the wild-type sequence in transient-transfection experiments (33). Moreover, a full-length NGFI-A construct incorporating this point mutation is resistant to repression by cotransfected NAB1 (34). Incorporation of this mutation into the NGFI-A R1/Gal4 DBD fusion disrupts its interaction in the yeast two-hybrid system with NCD1 of both

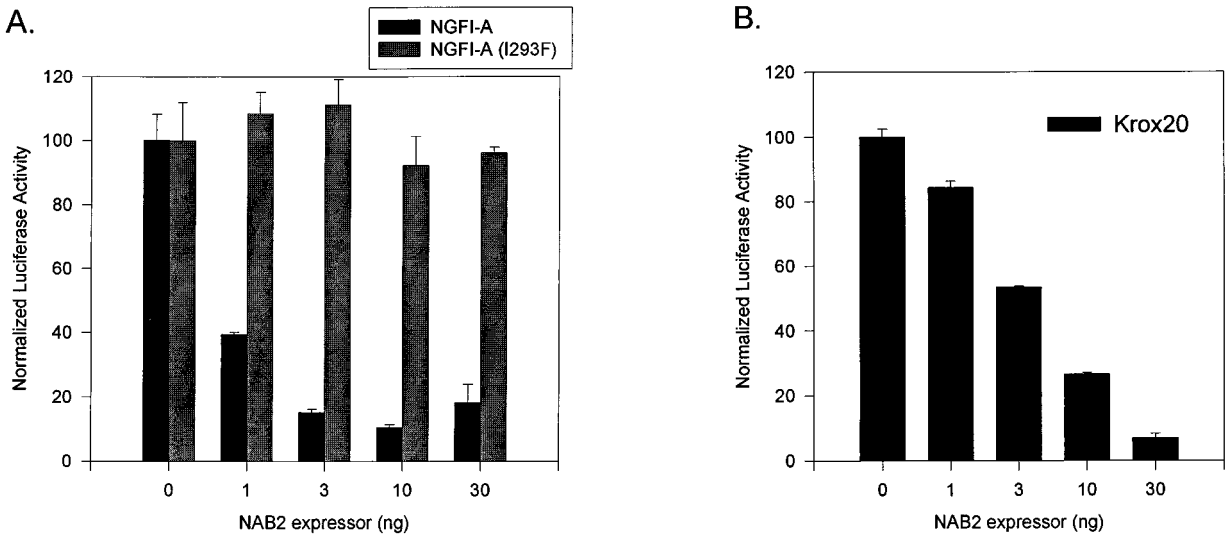

FIG. 3. NAB2 represses transactivation by NGFI-A and Krox20. CV-1 cells were transfected with plasmids expressing either wild-type NGFI-A, mutant NGFI-A (I293F) (A), or Krox20 (B), a luciferase reporter containing two upstream NGFI-A binding sites, and the indicated amounts of a plasmid expressing NAB2. Normalized luciferase activity is defined as the activity relative to NGFI-A [or NGFI-A (I293F) [A] or Krox20, [B]) in the absence of NAB2, which is set at 100%; activity of reporter alone is set at 0%. Means and standard deviations of two independent experiments are shown. Transfection assays using two independent plasmid preparations gave essentially identical results. Consistent with previous results (33, 34), the absolute activity of NGFI-A (I293F) in the absence of cotransfected NAB2 was more than 10-fold higher than that of wild-type NGFI-A. Transfection of higher amounts of NAB2 (100 ng) also failed to repress NGFI-A (I293F) activity (data not shown).

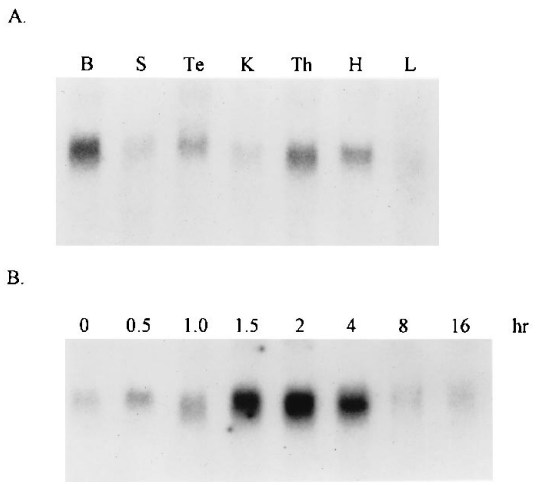

FIG. 4. Tissue specificity and regulation of NAB2 expression by NGF in PC12 cells. (A) An RNA blot of samples isolated from adult mouse brain (B), spleen (S), testes (Te), kidney (K), thymus (Th), heart (H), and liver (L) was hybridized with a ^{32}P-labeled DNA fragment derived from the mouse NAB2 cDNA. (B) PC12 cells were stimulated to differentiate by the addition of NGF (50 ng/ml), and RNA was isolated from nonstimulated cells (0 time point) and from cells exposed to NGF for the indicated times. An RNA blot of these samples was probed as described for panel A. The same blot was subsequently probed with cyclophilin, and normalization of the NAB2 signal to the amount of cyclophilin mRNA showed that NAB2 message increased ninefold 2 h after NGF addition.

NAB1 and NAB2 (Table 1). Disruption of NAB2 binding by the I293F point mutation in NGFI-A provides further evidence that the interaction between NAB2 and NGFI-A is specific.

Since NCD1 is well conserved in *C. elegans* NAB, we tested whether this domain was also capable of interacting with the NGFI-A R1 domain. As shown in Table 1, NCD1 of *C. elegans* NAB interacts with the NGFI-A R1 domain in the yeast two-hybrid system. Therefore, interactions between NAB homologs and proteins bearing R1-like domains are functionally conserved, presumably as a result of selective pressure to maintain such interactions throughout evolution.

NAB2 represses NGFI-A and Krox20. Because NAB2 was capable of interacting with NGFI-A, we proceeded to examine whether NAB2 could also repress NGFI-A transcriptional activity. The human NAB2 coding region was placed under the control of the CMV promoter and cotransfected with a plasmid expressing NGFI-A. NGFI-A activity, as measured using a luciferase reporter plasmid containing two NGFI-A binding sites fused to a minimal promoter, was repressed by NAB2 in a dose-dependent manner (Fig. 3A). This repression was not a global effect on transcription, because transcription of a *lacZ* reporter gene driven by either the Rous sarcoma virus or CMV promoter was unaffected by similar levels of NAB2 (data not shown). Like NAB1 (34), NAB2 failed to repress NGFI-A (I293F), demonstrating that repression of NGFI-A activity depends on an interaction between NAB2 and NGFI-A. To further compare NAB2 with NAB1, we tested the ability of NAB2 to repress transactivation by Krox20, a zinc finger protein that is closely related to NGFI-A. Similar to the results for NAB1 (34), NAB2 repressed transactivation by Krox20 (Fig. 3B).

Regulation of NAB2 expression. A low level of NAB1 mRNA expression is found in most tissues of the adult mouse (34). To determine whether NAB2 expression is similarly widespread, a blot of RNA samples isolated from various adult mouse tissues was hybridized with a probe for NAB2 (Fig. 4A). NAB2 mRNA is most highly expressed in the brain and thymus, with significant expression also in the spleen, kidney, heart, and testes. In contrast to NAB1, there appears to be little expression of NAB2 in the liver. The high levels of NAB2 mRNA in the brain and thymus are similar to the expression pattern of NGFI-A (50), indicating that NAB2 and NGFI-A are coexpressed in these tissues.

NGFI-A was originally identified as an immediate-early gene that is induced when PC12 cells are induced to differentiate by the addition of NGF (24). To test whether NAB2 expression is regulated by the same stimuli which activate NGFI-A expression, RNA was isolated from PC12 cells at several time points after NGF addition and an RNA blot was hybridized with a probe for NAB2 (Fig. 4B). The level of NAB2 mRNA increased approximately ninefold within 2 h after NGF addition. In contrast, probing the same blot for NGFI-A mRNA showed that it increased rapidly and peaked within 30 min after addition of NGF (data not shown) (5, 24, 42), demonstrating that the increase in NAB2 mRNA levels was delayed relative to the peak of NGFI-A expression. NAB1 mRNA was detected in PC12 cells, but its expression level did not appear to be regulated by NGF (data not shown).

Because mitogenic stimuli also rapidly increase NGFI-A levels (14), we tested whether NAB2 expression is similarly regulated by depriving NIH 3T3 fibroblasts of serum for 72 h and then inducing proliferation by the addition of 20% serum. As demonstrated previously (5, 18, 20), NGFI-A mRNA increased from virtually undetectable levels to very high levels of expression within 30 min after serum addition (Fig. 5A). NAB2 mRNA exhibited a threefold increase after 1 to 2 h of serum stimulation, and again the peak of expression was slightly delayed relative to that of NGFI-A mRNA. The level of NAB2 mRNA reproducibly decreased 4 h after serum stimulation and then eventually reached the steady-state level observed in cycling cells.

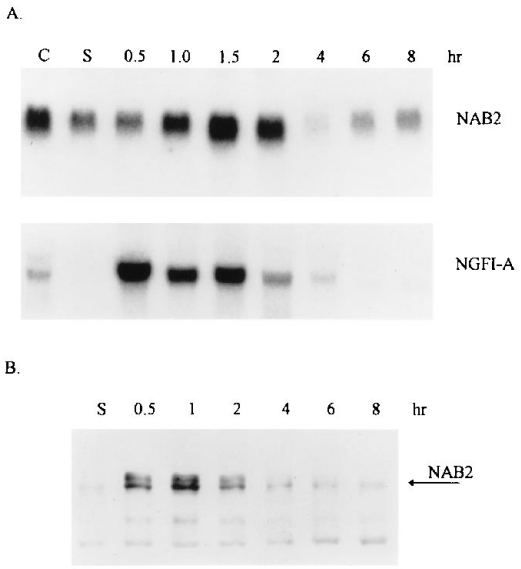

FIG. 5. NAB2 expression is stimulated by serum stimulation of NIH 3T3 fibroblasts. NIH 3T3 cells were starved of serum for 72 h and then stimulated by addition of 20% serum. Both RNA and protein were isolated from cycling, nonstarved cells (C), from serum-starved cells (S), and from serum-stimulated cells at the indicated time points. (A) An RNA blot of these samples was serially hybridized with probes for mouse NAB2 and for NGFI-A. The same blot was subsequently probed with cyclophilin, and normalization of the NAB2 signal to the amount of cyclophilin mRNA showed that NAB2 message increased threefold after serum stimulation. (B) A protein blot of these samples was probed with an affinity-purified rabbit anti-NAB2 antibody.

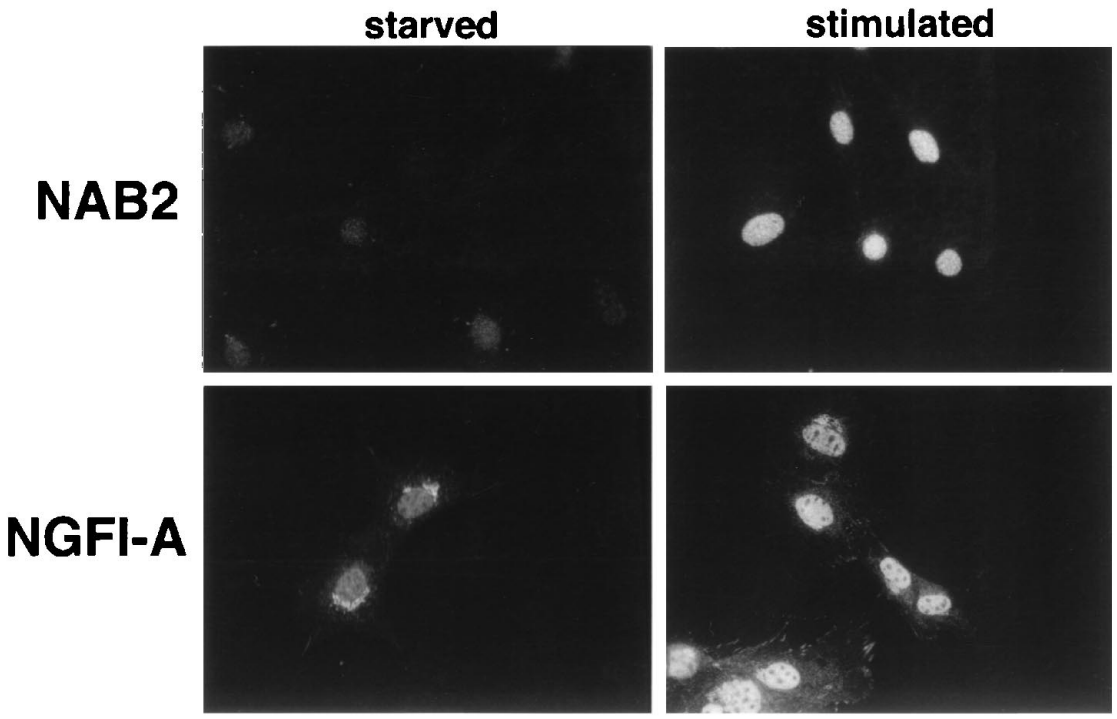

FIG. 6. Nuclear localization of NAB2. Serum-starved and serum-stimulated NIH 3T3 cells were fixed, permeabilized, and stained for endogenous NAB2 or NGFI-A as indicated. Protein levels of both NAB2 and NGFI-A are dramatically increased in the nucleus following serum stimulation. NGFI-A staining in starved cells is largely perinuclear, whereas the staining in stimulated cells appears to be both perinuclear and nuclear. Magnification is ×320.

To determine whether the modest increase in NAB2 mRNA observed in serum-stimulated NIH 3T3 cells was accompanied by a similar increase in NAB2 protein levels, we monitored NAB2 protein expression by using a polyclonal antibody raised against the NAB2 (147-161) peptide. A protein blot containing lysates isolated from NIH 3T3 cells at various times after serum stimulation demonstrated that the level of NAB2 protein increased dramatically after serum stimulation (Fig. 5B).

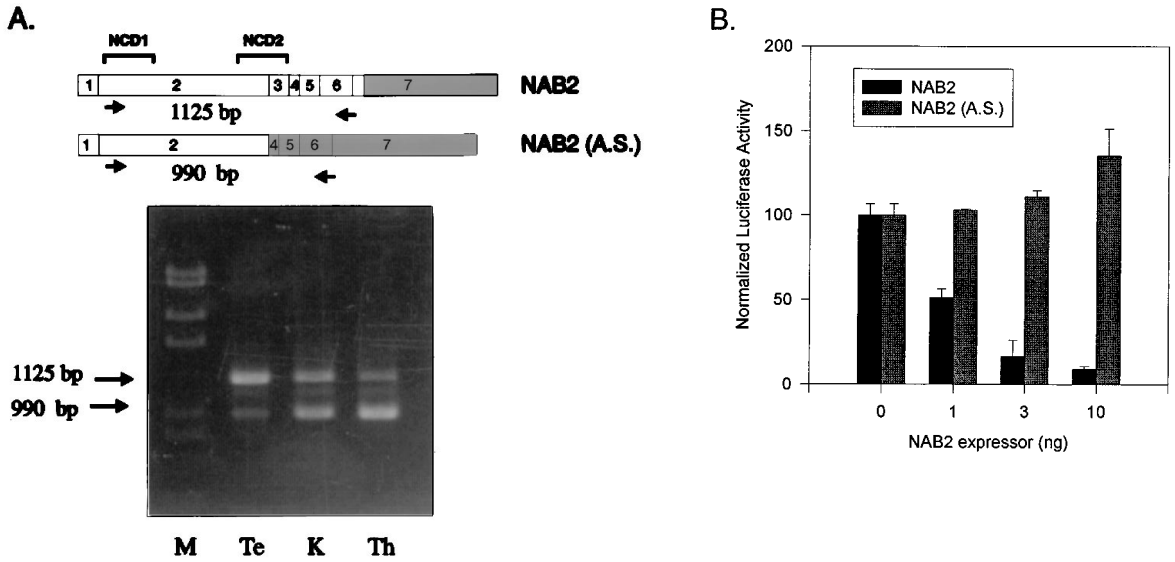

FIG. 7. NAB2 (A.S.) does not repress NGFI-A. (A) The exon structure contained within full-length and alternatively spliced NAB2 (A.S.) is shown at the top. NAB2 (A.S.) lacks a short 134-bp exon (exon 3) which lies just 3′ to the major exon that codes for the first 291 amino acids of full-length NAB2. Coding regions are shown by open boxes, and nontranslated regions are shaded. The alternative splice shifts the reading frame and results in a truncated protein product with the following C-terminal sequence: . . .RREGKQLSLHEASPstop. The ethidium bromide-stained agarose gel shows the PCR products obtained from cDNA isolated from mouse testes (Te), kidney (K), and thymus (Th), using the primers depicted in the diagram. The lane marked M contains molecular weight markers (*Hin*dIII-*Eco*RI-digested lambda DNA). (B) NAB2 (A.S.) was subcloned into the CMV-driven expression vector and was tested for its ability to repress transactivation by cotransfected NGFI-A. CV-1 cells were transfected with a plasmid expressing NGFI-A and the indicated amounts of plasmids expressing either NAB2 or NAB2 (A.S.). Normalized luciferase activity is defined as the activity relative to NGFI-A in the absence of NAB2, which is set at 100%; activity of reporter alone is set at 0%. Means and standard deviations of two independent experiments are shown. Transfection of higher amounts of NAB2 A.S. (100 ng) also failed to repress NGFI-A activity (data not shown).

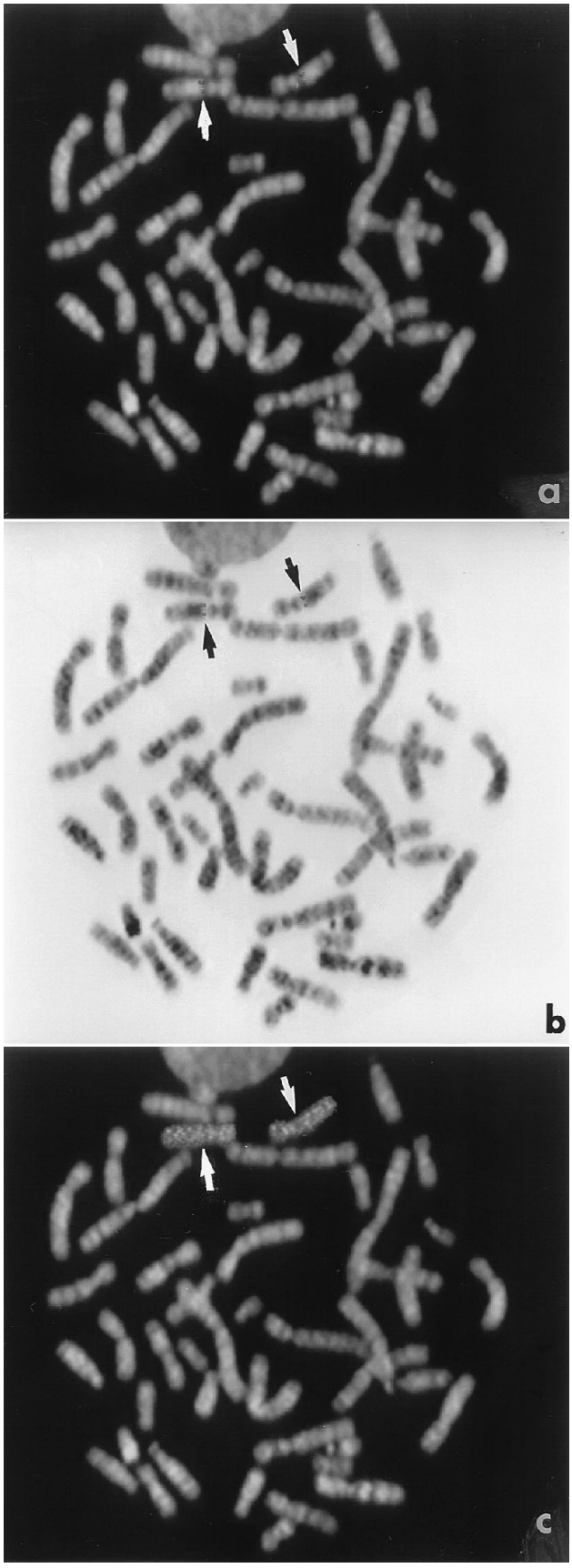

In fact, the induction of NAB2 protein was higher than would be predicted from the observed increase in NAB2 mRNA. Furthermore, the increase in NAB2 protein appeared to slightly precede the observed increase in the steady-state levels of NAB2 mRNA. Therefore, posttranscriptional regulation, such as increased protein stability or enhanced translation efficiency, may also be involved in the increase in NAB2 protein levels. NAB2 protein appears as a doublet on the gel, which could reflect phosphorylation of some of the potential kinase sites in the NAB2 sequence. Immunohistochemical analysis of serum-stimulated NIH 3T3 cells with the same antibody (Fig. 6) revealed an increased intensity of NAB2 staining after 1 h of serum stimulation, confirming the strong induction of NAB2 protein. These experiments also demonstrate that NAB2, like NGFI-A and NAB1 (22, 34), is principally localized in the nucleus.

NAB2 (A.S.) is unable to repress NGFI-A. Amplification of a DNA fragment containing the NAB2 ORF from mouse cDNA samples yielded PCR products of two different sizes (Fig. 7A). Aside from the expected fragment of 1,125 bp, a shorter PCR product of 990 bp was also present. Subcloning and sequencing of the shorter PCR fragment showed that it was derived from the NAB2 ORF but that it contained an internal deletion of 134 nucleotides. Analysis of the mouse NAB2 genomic sequence revealed that the deleted sequence constitutes an exon starting at amino acid 320 which is absent in the shorter NAB2 (A.S.) mRNA. Splicing out of this exon produces a frameshift that causes a premature termination of translation, resulting in the loss of approximately one-third of the NAB2 protein. A PCR survey of cDNA samples obtained from mouse tissues in which NAB2 is highly expressed shows that although both forms can be detected in every tissue examined, the ratio between them varies. For instance, the full-length form appears to predominate in the testis, whereas the shorter form is more abundant in the thymus (Fig. 7A). Similar analysis of human placental cDNA showed that a similar alternatively spliced form of human NAB2 mRNA exists in an approximately 1:1 ratio with the full-length product (data not shown).

Because the NAB2 (A.S.) mRNA has been detected in several tissues, we investigated the properties of its C-terminally truncated protein product. First, we tested its ability to repress in cotransfection experiments (Fig. 7B) and found that coexpression of increasing amounts of NAB2 (A.S.) failed to repress NGFI-A activity. Therefore, the removal of the exon results in production of a truncated protein which appears to be functionally distinct from full-length NAB2. Some preliminary evidence suggests that the C-terminal truncation may affect the subcellular localization of NAB2. Immunocytochemical staining of QT6 cells (quail fibroblast cell line) transfected with a construct expressing NAB2 (A.S.) resulted in production of protein which was no longer localized to the nucleus but rather appeared to be located in vesicular structures in the

FIG. 8. FISH localization of the NAB2 gene to human chromosomes. (a) Digital image of a metaphase chromosome spread derived from methotrexate-synchronized thymidine-released normal human peripheral leukocytes after FISH with a digoxigenin-labeled NAB2 probe and DAPI counterstaining. The symmetrical rhodamine signals on sister chromatids of chromosomes 12 are indicated by arrowheads. (b) The same metaphase showing a G-like banding pattern after the digital image of the DAPI-counterstained chromosomes was contrast enhanced and look-up-table inverted. The distinct banding pattern of individual chromosomes permits direct localization of the hybridization signal to band 12q13.3-14.1. (c) Rehybridization of the same spread with chromosome 12-painting probe confirms the identity of the labeled chromosomes (marked by arrowheads).

cytoplasm (1a). In contrast, a similar transfection of full-length NAB2 in QT6 cells showed nuclear staining of NAB2, consistent with the nuclear localization of NAB2 in NIH 3T3 cells (Fig. 6). Therefore, it seems that the C-terminal truncation of the protein produced by NAB2 (A.S.) mRNA adversely affects its nuclear localization and/or stability.

Chromosomal localization of the NAB2 gene. To obtain further clues regarding the function of NAB2, the chromosomal localization of human NAB2 was determined. Biotinylated or digoxigenin-labeled NAB2 genomic probes were hybridized to normal human chromosomes. Virtually all the metaphases had two homologous chromosomes, identified by banding and whole chromosome painting as chromosomes 12, with symmetrical fluorescent signal on the long arm at region q13-14 (Fig. 8). In both metaphases and prometaphases, the NAB2 gene was localized at region 12q13.3-14.1. This region is frequently rearranged in several solid tumors, lipomas, uterine leiomyomata, liposarcomas, gliomas, and phleomorphic adenomas of salivary glands (30, 37, 41, 47). In addition, region 12q13-15 is a preferential site for human papillomavirus integration in cervical carcinomas (28, 35). Microcell fusion-mediated transfer of this portion of chromosome 12 into a prostate cancer cell line has been shown to suppress its tumorigenicity (3).

DISCUSSION

The discovery of a second NAB molecule underscores the significance of these transcriptional corepressors and provides valuable clues to the functions of both proteins. Sequence conservation between NAB1 and NAB2 is concentrated within two discrete domains, whereas the remainder of the proteins have diverged considerably. Furthermore, NCD1 of either NAB1 or NAB2 is sufficient for interaction with NGFI-A. Since both NAB1 and NAB2 repress transcriptional activation mediated by NGFI-A and Krox20, NCD2 is a likely candidate for mediating transcriptional repression. A detailed structure-function analysis of NAB1 will be published elsewhere (43b).

Although NAB2 and NAB1 function similarly in cotransfection assays, some evidence suggests that NAB2 and NAB1 may play distinct physiological roles. Comparison of the expression patterns of NAB1 and NAB2 suggests that NAB2 activity is more closely linked to NGFI-A in vivo. Both NAB2 and NGFI-A are highly expressed in the thymus and brain, after NGF stimulation of PC12 cells, and after serum stimulation of fibroblasts. The massive induction and the subsequent rapid downregulation of NGFI-A after serum or NGF stimulation suggest that the transient nature of its expression is a critical aspect of its activity. Both NGFI-A mRNA and protein have very short half-lives, and their levels decrease rapidly after the initial burst of expression (14). The appearance of NAB2 could be yet another mechanism by which the initial burst of NGFI-A activity is quickly downregulated. The steady-state level of NAB2 protein decreases to basal levels after 4 h of serum stimulation, suggesting that it might also have a relatively short half-life. PEST domains have been implicated in decreasing protein stability (31), and the C terminus of NAB2 contains one such domain (residues 405 to 423).

A number of criteria have been used to characterize the activities of recently discovered corepressors, and the repression of NGFI-A by NAB1 and NAB2 exhibits a number of these properties. First, cotransfection of the corepressor leads to the specific neutralization of the transactivator with which it interacts (Fig. 3; references 16 and 34). Second, repression can be relieved by overexpression of the protein domain with which the corepressor interacts, presumably by titrating a limiting amount of endogenous corepressor. In this case, repression can again be restored if the level of the corepressor is augmented by transfection. This has been shown for the NGFI-A–NAB1 interaction (33) as well as for the repression of the retinoic acid and thyroid receptors by SMRT (7). Third, a point mutation in the transactivator which abrogates interaction with the corepressor (assayed either in vitro or in the yeast two-hybrid system) also renders the thyroid receptor or NGFI-A resistant to repression by N-CoR or NAB, respectively, in cotransfection experiments, (Fig. 3; references 16 and 34). Finally, recruitment of a corepressor to a minimal promoter exerts a repressive effect on basal transcription of that promoter. For example, fusion of the N-CoR and SMRT proteins with the Gal4 DBD represses activity of a basal promoter when Gal4 sites are placed upstream (7, 16). Similarly, fusion of the minimal R1 domain of NGFI-A to the Gal4 DBD represses basal transcription of a similar promoter construct, presumably through its recruitment of NAB1 and/or NAB2 (15).

In light of our results, analysis of the effects of NGFI-A and Krox20 in various contexts must take into account the potential contribution of NAB1 and NAB2. For example, it has previously been reported that NGFI-A activation of the thymidine kinase promoter is observed only if the cells are serum starved (25). One interpretation of this experiment is that endogenous levels of NGFI-A must be depleted (in this case, by serum starvation) before activation of the thymidine kinase promoter by exogenous NGFI-A can be observed. However, our experiments suggest another explanation, i.e., that reduction of endogenous NAB levels by serum starvation may be necessary to observe activation by cotransfected NGFI-A.

Sequencing of the *C. elegans* genome has identified a gene that is highly homologous to NAB1 and NAB2 within the two conserved domains. Interestingly, NCD1 of *C. elegans* NAB can mediate an interaction with the NGFI-A R1 domain in the yeast two-hybrid system. The rapid progress in sequencing the *C. elegans* genome (49) promises to facilitate the identification of NGFI-A homologs and other proteins which bear R1-like domains. The conservation of both sequence and function in *C. elegans* NAB strongly suggests that NAB proteins play a vital role in controlling fundamental processes such as cell division, differentiation, and/or apoptosis.

ACKNOWLEDGMENTS

We thank Mark Johnston for providing yeast strains and plasmids and Martin Rechsteiner for providing the PESTFIND program. We are also indebted to Alex Swirnoff and Steve Lee for advice and critical comments on the manuscript.

J.S. was supported by NIH grant T32-DK07296, B.R.S. was supported by NIH grant T32-GM07067, and E.D.A. was supported by a fellowship from the American Heart Association, Missouri Affiliate. This work was supported by grant PO1 CA49712 from the National Cancer Institute and by a grant from The Association for the Cure of Cancer of the Prostate (CaP CURE). J.M. is an Established Investigator of the American Heart Association.

REFERENCES

1. **Altschul, S. F., W. Gish, W. Miller, E. W. Myers, and D. J. Lipman.** 1990. Basic local alignment search tool. J. Mol. Biol. **215:**403–410.
1a. **Apel, E.** Unpublished data.
2. **Bairoch, A.** 1993. The Prosite dictionary of sites and patterns in proteins, its current status. Nucleic Acids Res. **21:**3097–3103.
3. **Bérubé, N. G., M. D. Speevak, and M. Chevrette.** 1994. Suppression of tumorigenicity of human prostate cancer cells by introduction of human chromosome del(12)(q13). Cancer Res. **54:**3077–3081.
4. **Brewer, C. B.** 1994. Cytomegalovirus plasmid vectors for permanent lines of polarized epithelial cells. Methods Cell Biol. **43:**233–245.
5. **Cao, X., R. A. Koski, A. Gashler, M. McKiernan, C. F. Morris, R. Gaffney, R. V. Hay, and V. K. Sukhatme.** 1990. Identification and characterization of the *EGR-1* gene product, a DNA-binding zinc finger protein induced by

differentiation and growth signals. Mol. Cell. Biol. **10:**1931–1939.
6. **Changelian, P. S., P. Feng, T. C. King, and J. Milbrandt.** 1989. Structure of the NGFI-A gene and detection of upstream sequences responsible for its transcriptional induction by nerve growth factor. Proc. Natl. Acad. Sci. USA **86:**377–381.
7. **Chen, J. D., and R. M. Evans.** 1995. A transcriptional co-repressor that interacts with nuclear hormone receptors. Nature (London) **377:**454–457.
8. **Christy, B. A., L. F. Lau, and D. Nathans.** 1988. A gene activated in mouse 3T3 cells by serum growth factors encodes a protein with "zinc finger" sequences. Proc. Natl. Acad. Sci. USA **85:**7857–7861.
9. **Day, M. L., T. J. Fahrner, S. Ayken, and J. Milbrandt.** 1990. The zinc finger protein NGFI-A exists in both nuclear and cytoplasmic forms in nerve growth factor-stimulated PC12 cells. J. Biol. Chem. **265:**15253–15260.
10. **Durfee, T., K. Becherer, P. Chen, S. Yeh, Y. Yang, A. E. Kilburn, W. Lee, and S. J. Elledge.** 1993. The retinoblastoma protein associates with the protein phosphatase type 1 catalytic subunit. Genes Dev. **7:**555–569.
11. **Fields, S.** 1993. The two-hybrid system to detect protein-protein interactions. Methods (Orlando) **5:**116–124.
12. **Fields, S., and R. Sternglanz.** 1994. The two-hybrid system: an assay for protein-protein interactions. Trends Genet. **10:**286–292.
13. **Frohman, M. A.** 1993. Rapid amplification of complementary DNA ends for generation of full-length complementary DNAs: thermal RACE. Methods Enzymol. **218:**340–356.
14. **Gashler, A., and V. P. Sukhatme.** 1995. Early growth response protein 1 (Egr-1): prototype of a zinc-finger family of transcription factors. Prog. Nucleic Acid Res. Mol. Biol. **50:**191–224.
15. **Gashler, A. L., S. Swaminathan, and V. P. Sukhatme.** 1993. A novel repression module, an extensive activation domain, and a bipartite nuclear localization signal defined in the immediate-early transcription factor Egr-1. Mol. Cell. Biol. **13:**4556–4571.
16. **Hörlein, A. J., A. M. Naar, T. Heinzel, J. Torchia, B. Gloss, R. Kurokawa, A. Ryan, Y. Kamei, M. Soderstrom, C. K. Glass, and M. G. Rosenfeld.** 1995. Ligand-independent repression by the thyroid hormone receptor mediated by a nuclear receptor co-repressor. Nature (London) **377:**397–404.
17. **Krishnaraju, K., H. Q. Nguyen, D. A. Liebermann, and B. Hoffman.** 1995. The zinc finger transcription factor Egr-1 potentiates macrophage differentiation of hematopoietic cells. Mol. Cell. Biol. **15:**5499–5507.
18. **Lau, L. F., and D. Nathans.** 1987. Expression of a set of growth-related immediate early genes in BALB/c 3T3 cells: coordinate regulation with c-fos or c-myc. Proc. Natl. Acad. Sci. USA **84:**1182–1186.
19. **Lee, S. L., Y. Sadovsky, A. H. Swirnoff, P. Goda, and J. Milbrandt.** Submitted for publication.
20. **Lemaire, P., O. Revelant, R. Bravo, and P. Charnay.** 1988. Two mouse genes encoding potential transcription factors with identical DNA-binding domains are activated by growth factors in cultured cells. Proc. Natl. Acad. Sci. USA **85:**4691–4695.
21. **Liu, J., T. E. Wilson, J. Milbrandt, and M. Johnston.** 1993. Identifying DNA-binding sites and analyzing DNA-binding domains using a yeast selection system. Methods (Orlando) **5:**125–137.
22. **Matheny, C., M. L. Day, and J. Milbrandt.** 1994. The nuclear localization signal of NGFI-A is located within the zinc finger DNA binding domain. J. Biol. Chem. **269:**8176–8181.
23. **Milbrandt, J.** 1986. Nerve growth factor rapidly induces c-fos mRNA in PC12 rat pheochromocytoma cells. Proc. Natl. Acad. Sci. USA **83:**4789–4793.
24. **Milbrandt, J.** 1987. A nerve growth factor-induced gene encodes a possible transcriptional regulatory factor. Science **238:**797–799.
25. **Molnar, G., A. Crozat, and A. B. Pardee.** 1994. The immediate-early gene *Egr-1* regulates the activity of the thymidine kinase promoter at the G_0-to g_1 transition of the cell cycle. Mol. Cell. Biol. **14:**5242–5248.
26. **Muthukumar, S., P. Nair, S. F. Sells, N. G. Maddiwar, R. J. Jacob, and V. M. Rangnekar.** 1995. Role of Egr-1 in thapsigargin-inducible apoptosis in the melanoma cell line A375-C6. Mol. Cell. Biol. **15:**6262–6272.
27. **Paulsen, R. E., C. A. Weaver, T. J. Fahrner, and J. Milbrandt.** 1992. Domains regulating transcriptional activity of the inducible orphan receptor NGFI-B. J. Biol. Chem. **267:**16491–16496.
28. **Popescu, N., S. C. Amsbaugh, and J. A. DiPaolo.** 1987. Human papillomavirus type 18 DNA is integrated at a single chromosome site in cervical carcinoma cell line SW756. J. Virol. **61:**1682–1685.
29. **Popescu, N., D. Zimonjic, C. Hatch, and W. Bonner.** 1994. Chromosomal mapping of the human histone gene H2AZ to 4q24 by fluorescence in situ hybridization. Genomics **20:**333–335.
30. **Reifenberger, G., J. Reifenberger, K. Ichimura, and V. P. Collins.** 1995. Amplification at 12q13-14 in human malignant gliomas is frequently accompanied by loss of heterozygosity at loci proximal and distal to the amplification site. Cancer Res. **55:**731–734.
31. **Rogers, S., R. Wells, and M. Rechsteiner.** 1986. Amino acid sequences common to rapidly degraded proteins: the PEST hypothesis. Science **234:**364–368.
32. **Rose, M. S., F. Winston, and P. Hieter.** 1990. Methods in yeast genetics: a laboratory course manual. Cold Spring Harbor Press, Cold Spring Harbor, N.Y.
33. **Russo, M. W., C. Matheny, and J. Milbrandt.** 1993. Transcriptional activity of the zinc finger protein NGFI-A is influenced by its interaction with a cellular factor. Mol. Cell. Biol. **13:**6858–6865.
34. **Russo, M. W., B. R. Sevetson, and J. Milbrandt.** 1995. Identification of NAB1, a repressor of NGFI-A and Krox20 mediated transcription. Proc. Natl. Acad. Sci. USA **92:**6873–6877.
35. **Sastre-Garau, X., S. Schneider-Maunoury, J. Couturier, and G. Orth.** 1990. Human papillomavirus type 16 DNA is integrated in chromosome region 12q14-q15 in a cell line derived from a vulvar intraepithelial neoplasia. Cancer Genet. Cytogenet. **44:**253–261.
36. **Schneider-Maunoury, S., P. Topilko, T. Seitanidou, G. Levi, M. Cohen-Tannoudji, S. Pournin, C. Babinet, and P. Charnay.** 1993. Disruption of Krox-20 results in alteration of rhombomeres 3 and 5 in the developing hindbrain. Cell **75:**1199–1214.
37. **Schoenberg Fejzo, M., S. Yoon, K. T. Montgomery, M. S. Rein, S. Weremowicz, K. S. Krauter, T. E. Dorman, J. A. Fletcher, J. Mao, D. T. Moir, R. S. Kucherlapati, and C. C. Morton.** 1995. Identification of a YAC spanning the translocation breakpoints in uterine leiomyomata, pulmonary chondroid hamartoma, and lipoma: physical mapping of the 12q14-15 breakpoint region in uterine leiomyomata. Genomics **26:**265–271.
38. **Sells, S. F., S. Muthukumar, V. P. Sukhatme, S. A. Crist, and V. M. Rangnekar.** 1995. The zinc finger transcription factor Egr-1 impedes interleukin-1-inducible tumor growth arrest. Mol. Cell. Biol. **15:**682–692.
39. **Seyfert, V. L., S. B. McMahon, W. D. Glenn, A. J. Yellen, V. P. Sukhatme, X. Cao, and J. G. Monroe.** 1990. Methylation of an immediate-early inducible gene as a mechanism for B cell tolerance induction. Science **250:**797–800.
40. **Seyfert, V. L., V. P. Sukhatme, and J. G. Monroe.** 1989. Differential expression of a zinc finger-encoding gene in response to positive versus negative signaling through receptor immunoglobulin in murine B lymphocytes. Mol. Cell. Biol. **9:**2083–2088.
41. **Solomon, E., J. Borrow, and A. D. Goddard.** 1991. Chromosome aberrations and cancer. Science **254:**1153–1160.
42. **Sukhatme, V. P., X. Cao, L. C. Chang, C. H. Tsai-Morris, D. Stamenkovich, P. C. P. Ferreira, D. R. Cohen, S. A. Edwards, T. B. Shows, T. Curran, M. Le Beau, and E. D. Adamson.** 1988. A zinc finger-encoding gene coregulated with c-fos during growth and differentiation, and after cellular depolarization. Cell **53:**37–43.
43. **Suva, L. J., M. Ernst, and G. A. Rodan.** 1991. Retinoic acid increases *zif268* early gene expression in rat preosteoblastic cells. Mol. Cell. Biol. **11:**2503–2510.
43a. **Svaren, J., and J. Milbrandt.** Unpublished data.
43b. **Swirnoff, A., and J. Milbrandt.** Unpublished data.
44. **Topilko, P., S. Schneider-Maunoury, G. Levi, A. Baron-Van Evercooren, A. B. Y. Chennoufi, T. Seitanidou, C. Babinet, and P. Charnay.** 1994. Krox-20 controls myelination in the peripheral nervous system. Nature (London) **371:**796–799.
45. **Treitel, M. A., and M. Carlson.** 1995. Repression by SSN6-TUP1 is directed by MIG1, a repressor/activator protein. Proc. Natl. Acad. Sci. USA **92:**3132–3136.
46. **Tzamarias, D., and K. Struhl.** 1994. Functional dissection of the yeast Cyc8-Tup1 transcriptional c8-repressor complex. Nature (London) **369:**758–761.
47. **Van de Ven, W. J. M., E. F. P. M. Schoenmakers, S. Wanschura, B. Kazmierczak, P. F. J. Kools, J. M. W. Geurts, S. Bartnitzke, H. Van den Berghe, and J. Bullerdiek.** 1995. Molecular characterization of MAR, a multiple aberration region on human chromosome segment 12q13-q15 implicated in various solid tumors. Genes Chromosomes Cancer **12:**296–303.
48. **Varnum, B. C., R. W. Lim, D. A. Kujubu, S. J. Luhner, S. E. Kaufman, J. S. Greenberger, J. C. Gasson, and H. R. Herschman.** 1989. Granulocyte-macrophage colony-stimulating factor and tetradecanoyl phorbol acetate induce a distinct, restricted subset of primary-response *TIS* genes in both proliferating and terminally differentiated myeloid cells. Mol. Cell. Biol. **9:**3580–3583.
49. **Waterston, R., and J. Sulston.** 1995. The genome of Caenorhabditis elegans. Proc. Natl. Acad. Sci. USA **92:**10836–10840.
50. **Watson, M. A., and J. Milbrandt.** 1990. Expression of the nerve growth factor-regulated NGFI-A and NGFI-B genes in the developing rat. Development **110:**173–183.
51. **Weinberg, R. A.** 1995. The retinoblastoma protein and cell cycle control. Cell **81:**323–330.
52. **Weintraub, S. J., K. N. B. Chow, R. X. Luo, S. H. Zhang, S. He, and D. C. Dean.** 1995. Mechanism of active transcriptional repression by the retinoblastoma protein. Nature (London) **375:**812–815.
53. **Xu, J., and N. Wang.** 1994. Identification of chromosomal structural alterations in human ovarian carcinoma cells using combined GTG-banding and repetitive fluorescence in situ hybridization (FISH). Cancer Genet. Cytogenet. **74:**1–7.
54. **Zimonjic, D. B., N. C. Popescu, T. Matsui, M. Ito, and K. Chihara.** 1994. Localization of the human cholecystokinin-B/gastrin receptor gene (CCKBR) to chromosome 11p15.5-p15.4 by fluorescence in situ hybridization. Cytogenet. Cell Genet. **65:**184–185.
55. **Zimonjic, D. B., L. Rezanka, J. A. DiPaolo, and N. C. Popescu.** 1995. Refined localization of the erbB-3 proto-oncogene by direct visualization of FISH signals on LUT-inverted and contrast-enhanced digital images of DAPI-banded chromosomes. Cancer Genet. Cytogenet. **80:**100–102.